

Variational Quantum-Neural Hybrid Error Mitigation

Shi-Xin Zhang,^{1,2} Zhou-Quan Wan,^{1,2} Chang-Yu Hsieh,^{2,*} Hong Yao,^{1,†} and Shengyu Zhang^{2,‡}

¹*Institute for Advanced Study, Tsinghua University, Beijing 100084, China*

²*Tencent Quantum Laboratory, Tencent, Shenzhen, Guangdong 518057, China*

(Dated: December 21, 2021)

Quantum error mitigation (QEM) is crucial for obtaining reliable results on quantum computers by suppressing quantum noise with moderate resources. It is a key for successful and practical quantum algorithm implementations in the noisy intermediate scale quantum (NISQ) era. Since quantum-classical hybrid algorithms can be executed with moderate and noisy quantum resources, combining QEM with quantum-classical hybrid schemes is one of the most promising directions toward practical quantum advantages. In this paper, we show how the variational quantum-neural hybrid eigensolver (VQNHE) algorithm, which seamlessly combines the expressive power of a parameterized quantum circuit with a neural network, is inherently noise resilient with a unique QEM capacity, which is absent in vanilla variational quantum eigensolvers (VQE). We carefully analyze and elucidate the asymptotic scaling of this unique QEM capacity in VQNHE from both theoretical and experimental perspectives. Finally, we consider a variational basis transformation for the Hamiltonian to be measured under the VQNHE framework, yielding a powerful tri-optimization setup that further enhances the quantum-neural hybrid error mitigation capacity.

Introduction. Variational quantum algorithms (VQA) [1–3] are under active investigations as they require moderate quantum hardware resources and are promising candidates to deliver practical quantum advantage [4, 5] in the NISQ era [6]. VQE is one of the most representative VQAs where the ground state is approximated by variational optimization [7–13] with parameterized quantum circuits. Quantum error mitigation, as a NISQ alternative for full-fledged quantum error correction, is believed to alleviate the negative effects brought by the quantum noise and deliver more reliable results for VQAs. There are already various proposals for QEM techniques [14–27] and specifically some of the proposals are based on the principle of variational optimizations [28–37]. However, the interplay in terms of variational optimization between VQA and QEM remains largely elusive so far. To pave a way toward more practical quantum advantages, it is natural and urgent to investigate the interplay between VQAs and QEM as well as design VQA-native QEM techniques or QEM baked-in VQAs.

Variational quantum-neural hybrid eigensolver (VQNHE) is a powerful VQA approach incorporating the strength of a neural network as a nonunitary post-processing module efficiently [38]. Recently, the idea of adding a non-unitary processing module to the variational quantum eigensolver [7–12] has become popular. However, unlike all previous proposals, VQNHE not only enhances the expressive power of the VQAs but also entails just a polynomial scaling of resource overhead. For instance, while a previous proposal based on the Jastrow factor [39] could enhance VQE approach [40, 41] it requires an exponential scaling of resources overhead for the general form of Jastrow factor. In this work, we reveal another important property of VQNHE: the intrinsic noise resilience. Through detailed analyses, we demonstrate that this unique quantum noise resilience is

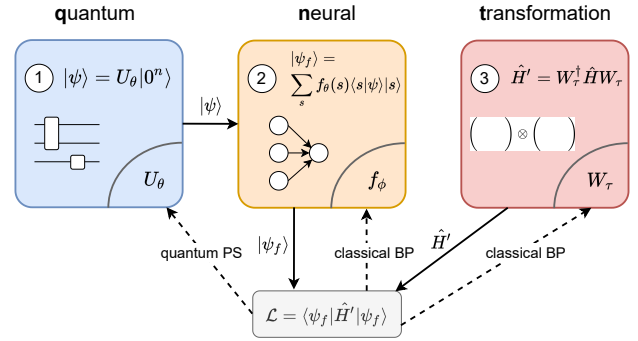


FIG. 1. Schematic workflow for the transformed Hamiltonian approach combined with VQNHE. The dashed lines are for gradient descent where the gradients are obtained from quantum parameter shift (PS) and classical backpropagation (BP), respectively. This tri-optimization setup further enhance the expressive power and the error resilience compared to VQNHE.

due to the introduction of the classical post-processing module and such QEM capacity is absent in the plain VQE. By utilizing the simple idea of adaptive retraining on noisy hardware, we obtain much more reliable energy estimations in the presence of quantum noise. In addition, by introducing the transformed Hamiltonian approach as shown in Fig. 1, we further improve the expressive power and the noise resilience of VQNHE, rendering a more efficient and reliable approach for quantum simulation on noisy hardware.

VQNHE setup. We first recapitulate the essence of VQNHE and then elaborate on *adaptive retraining*, a QEM setup built on top of VQNHE. VQNHE is an interesting example of quantum-classical hybrid schemes: It not only requires an outer classical optimizer loop but also features a classical neural network to provide the post-processing enhancement. The aim of VQNHE is

the same as VQE, i.e. to find the ground state of a given Hamiltonian H . To approximate such a ground state, we do not directly rely on the output state of a parameterized quantum circuit (PQC) U as $|\psi\rangle = U|0\rangle$. Instead, we post-process the output of a PQC with a classical neural network to attain $|\psi_f\rangle = \hat{f}|\psi\rangle$. Here $\hat{f} = \sum_s f(s)|s\rangle\langle s|$, where f is a neural network with trainable weights and s is a computational basis. We note that the neural network f can generally induce nonunitary transformation on the quantum state, and it was widely believed that the experimental implementation for accurate estimations on the energy $\langle\psi_f|\hat{H}|\psi_f\rangle$ requires exponential time. However, as explicated in an earlier work [38], this energy estimation for VQNHE can be accurately and efficiently obtained with only a polynomial scaling of hardware resources as given by:

$$\langle\hat{H}\rangle_{\psi_f} = \frac{\langle(1-2s_0)f(0s_{1:n-1})f(1\widetilde{s_{1:n-1}})\rangle_{UV}}{\langle f(s)^2 \rangle_U}, \quad (1)$$

where the bitstring s in the denominator is drawn from the PQC U and bitstring \tilde{s} in the numerator is drawn from the PQC with the measurement circuit V appended (See [38] for the construction details of measurement circuit V) and \tilde{s} is for bitstring with bit-flip on s .

In summary, VQNHE jointly optimizes the parameters in the PQC U and the neural network post-processing module f . As an approach combining the advantages from both VQE and neural variational Monte Carlo (VMC) [42–48], this new setup offers a state-of-the-art approximation on the ground state energy for various quantum spin systems and quantum molecules with a provable bound on the efficiency for the resource overhead [38].

Retraining energy as a measure for QEM capacity. We investigate the VQNHE performance on both noisy quantum simulators and the real quantum hardware. The quantum noise deteriorates the accuracy of the energy estimation and thus compromises the superior performance that could be attained in an ideal situation, such as a noise-free simulation. Interestingly, we find that VQNHE exhibits an inherent noise resilience to certain extent. Namely, when training the VQNHE in a noisy environment, the neural network can adjust its weights, implicitly mitigating noise-induced disruptions. We term the optimization on noisy hardware the *adaptive retraining*. The QEM capacity of VQNHE can be measured by the difference of energy estimations $\delta E = E_\phi - E_{\phi_0}$, where E_ϕ is the energy estimation with neural weights ϕ , and ϕ_0 is the optimized weights with(out) the presence of quantum noise. Apart from the neural retraining, we can also investigate the energy gain when retraining the PQC or jointly retraining the PQC and the neural network. The energy gains are defined as $\delta E = E_\theta - E_{\theta_0}$ and $\delta E = E_{\theta,\phi} - E_{\theta_0,\phi_0}$, respectively, where θ_0 is the set of optimized parameters in the PQC trained with(out) noise. It is worth noting that

the so-called retraining can start from any weight initializations, especially in the joint retraining case. The noiseless optimal parameters are only used to define the energy gain theoretically, and are not necessary for the practical QEM.

Biased retraining on the classical module. In real experiments, the energy is estimated from a collection of measured bitstrings with finite sampling errors. The number of measurement shots required is often large, especially when near optimum or due to the barren plateaus [49–51]. Therefore, it is expensive to run full unbiased retraining. To this end, we propose a very cost-efficient alternative, i.e. biased retraining, which implies only retraining the neural network. In the biased retraining, instead of executing the PQC at each epoch, we fix the bitstring results during the retraining. Since the bitstring results are fixed (with just a finite number of shots), they are biased with measurement uncertainty. As a result, the obtained biased retraining energy gain has two components: the intrinsic QEM and an overfitting to the biased measurements. With noisy simulations and real IBM hardware experiments, we show that the average QEM capacity scaling for the biased neural retraining is $\delta E \propto B + A/M$ where M is the number of fixed measurement shots and the constant B stands for intrinsic QEM. (See the SM for the details.)

QEM capacity scaling with the noise strength.

To investigate the energy gain with a tunable noise strength, we utilize a simple depolarizing error model, where an isotropic depolarization of strength p is attached after each two-qubit gate. The one-dimensional five-site transverse field Ising model (TFIM) with an open boundary condition is then utilized as the VQNHE target Hamiltonian: $\hat{H} = \sum_{i=1}^{n-1} Z_i Z_{i+1} - \sum_{i=1}^n X_i$. We study the scaling relation between the energy gain due to the intrinsic QEM and the effective overall noise strength p_{eff} of the depolarization. The overall depolarizing probability p_{eff} is measured by the energy ratio from the PQC output: $1 - p_{\text{eff}} = E_{\text{noise}}/E_{\text{noiseless}}$. For depolarizing strength $p = 0.005, 0.01, 0.015, 0.02$, the effective overall error strength are correspondingly $p_{\text{eff}} = 0.017, 0.033, 0.049, 0.065$ with our circuit ansatz and the intrinsic QEM energy gain from neural retraining are $\delta E = -0.0031, -0.012, -0.026, -0.044$, respectively. The scaling relation for the QEM energy gain with neural retraining is thus given by $\delta E \propto p_{\text{eff}}^2$.

Note that the intrinsic QEM capacity scales quadratically with p_{eff} , which leads to the biased neural retraining scaling with the number of measurements. Note that the effect of finite sampling errors, where the real overall noise strength p_{eff} can only be approximately estimated in experiments. We take p_{eff} as a random variable and the energy gain is $\delta E \propto \langle p_{\text{eff}}^2 \rangle = \langle p_{\text{eff}} \rangle^2 + \Delta p_{\text{eff}}$, where $\Delta p_{\text{eff}} \propto 1/M$ is the square deviation of the estimation on p_{eff} . Therefore, the energy gain after retraining follows a simple scaling form of $A/M + B$ as we have shown before.

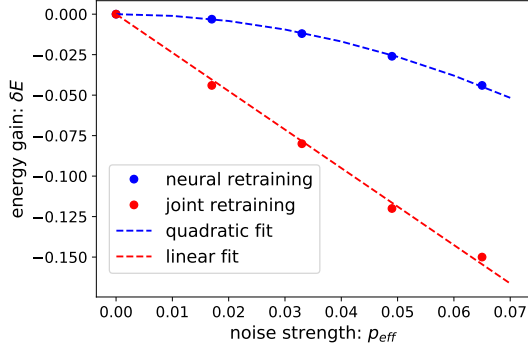


FIG. 2. Scaling between retraining energy gain and the noise strength. The system is five-qubit TFIM and the underlying error model is depolarizing noise. The QEM capacity due to neural retraining is quadratic with the noise strength and is thus much weaker than joint retraining, which has linear scaling against the noise strength.

In addition, we evaluate the QEM energy gain from joint retraining, with $\delta E = -0.044, -0.080, -0.12, -0.15$ for effective error strengths listed above. Therefore, the scaling of QEM capacity with the quantum noise strength from joint retraining is linear instead of quadratic: $\delta E \propto p_{\text{eff}}$. The different scaling forms are sketched in Fig. 2 for both neural retraining and joint retraining.

General picture for the QEM scaling. To understand the above QEM scaling relations, we first investigate a minimal model involving just one qubit which permits direct analytical analysis. The results are consistent with the observed scaling relation (see SM for details).

We now discuss the theoretical mechanism behind different QEM capacity scalings. Suppose that the ideal output of a PQC is the exact ground state as $\rho_0 = |\psi_0\rangle\langle\psi_0|$. And the mixed state from the PQC in the presence of depolarizing noise of strength p is ρ . The post-processing module is a nonunitary transformation \hat{f} with non-zero elements only appearing in the diagonal. The energy gain with neural retraining is thus $\delta E = E_{QEM} - E_N$. Here $E_N = (1-p)E_0$ where $E_0 = \text{Tr}(\rho_0 H)$ is for the exact ground state. We expand the energy terms as $E_{QEM} = E_{QEM}^{(0)} + E_{QEM}^{(1)}p + E_{QEM}^{(2)}p^2 + \dots$ and keep up to the first order of p , namely, as long as we have shown that the zeroth and first order of p in the energy gain is zero, the energy gain scaling is at most p^2 .

Under depolarizing channel p , we have:

$$E_{QEM} = \frac{\text{Tr}(\hat{f}\rho_0\hat{f}\hat{H})(1-p) + \text{Tr}(\hat{f}\hat{H}\hat{f})p/2^n}{p + \text{Tr}(\hat{f}\rho_0\hat{f})(1-p)}. \quad (2)$$

The optimized neural module $f = I$ when $p = 0$. We assume the optimized $f \approx I + pf_1$ to the first order, where f_1 is a constant matrix.

The zeroth order of p in the energy gain is trivially zero: $E_{QEM}^{(0)} = E_0$. Now consider the first order of p ,

and we have $E_N^{(1)} = -E_0$ and

$$E_{QEM}^{(1)} = \text{Tr}(f_1\rho_0 H) - E_0\text{Tr}(f_1\rho_0) + \text{Tr}(\rho_0 f_1 H) - E_0\text{Tr}(\rho_0 f_1) - E_0. \quad (3)$$

Note that

$$\text{Tr}(f_1\rho_0 H) - E_0\text{Tr}(f_1\rho_0) = \langle\psi_0|Hf_1|\psi_0\rangle - E_0\langle\psi_0|f_1|\psi_0\rangle = 0 \quad (4)$$

thus we have $E_{QEM}^{(1)} = -E_0$, independent of f_1 . Therefore, the first order energy gain vanishes $\delta E^{(1)} = 0$ as well, indicating that the energy gain scales at most quadratically with the noise strength p . To summarize, the first order of p in the energy gain is canceled as long as the retraining trajectory can be understood from a simple perturbation, i.e. the optimized post-processing module f is analytically connected to the ideal one I as the noise $p \rightarrow 0$.

To explain why a linear gain emerges in the joint retraining, we note that the perturbative picture fails under the joint-training scenario. As long as we allow joint training, there are infinitely many optimal solutions, constituted by appropriate combinations of PQC and neural-network adjustments to essentially yield the same output state in the noiseless case. We are no longer restricted to the unique solution as in the neural retraining case, where the PQC generates the exact ground state with an identity NN. Instead, even when the PQC generates other quantum states than the true ground state, an appropriate post-processing neural module f can still post-process and lead to the ground truth. Therefore, in the ideal case $p = 0$, we have infinitely many combinations of PQC states and neural solutions that would collaboratively lead to the correct ground state energy. When noise $p > 0$ is introduced, the responses to quantum noise are different and the energy degeneracy (of many possible combinations of PQC and NN setups) is broken. Note that the optimal solution is not the identity one $f = I$. In other words, the optimized f cannot be simply described by $f = I + pf_1$ where the derivation based on the perturbation picture fails and the first order energy gain emerges.

In summary, the energy gains in neural retraining and joint retraining come from different sources. The neural retraining perturbatively improves the noisy energy estimation by smoothly shifting the classical module f away from identity I . On the contrary, the joint retraining improves the energy estimation by breaking the degeneracy of infinitely many possible combinations of PQC and neural setups and selecting the most error-resilient one.

Tri-optimization with parameterized transformed Hamiltonian. VQNHE is a bi-optimization setup, where both parameters θ in the PQC and parameters ϕ in the neural network need to be optimized. The post-processing function f can greatly alter the output

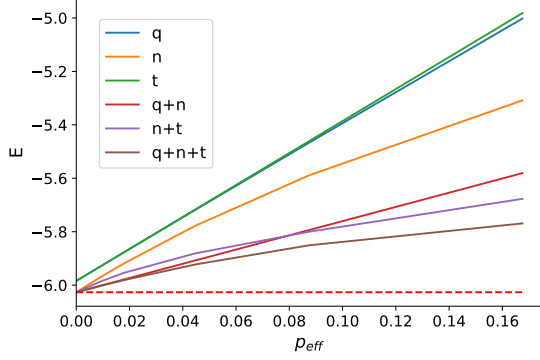


FIG. 3. Energy estimation for five-qubit TFIM on noisy hardware with different adaptive retraining schemes. The depolarizing noise strength is characterized by $p_{\text{eff}} = 1 - E_n/E_0$, where E_n (E_0) is energy estimation with(out) noise. Here q is for retraining on the PQC part, n is for retraining on the neural network part and t is for retraining on the parameterized gauge transformation part. We omit the result of no retraining and $q+t$ as they are both similar to retraining PQC (q). The dashed red line indicates the exact ground state energy.

states by the PQC. However, \hat{f} is effectively a diagonal matrix, which certainly cannot represent a universal quantum channel. Therefore, such retraining of the neural post-processing module can only partially mitigate the quantum noise effects. Since a universal quantum channel is NP hard to implement in terms of quantum resources, we instead introduce a parameterized gauge Hamiltonian approach to enhance the mitigating power of the post-processing quantum channel \hat{f} .

Suppose that \hat{W} is a unitary transformation, then the transformed Hamiltonian $\hat{H}' = \hat{W}^\dagger \hat{H} \hat{W}$ shares the identical spectrum with \hat{H} , and thus the ground state energy is the same as that of \hat{H} . Therefore, we can utilize VQNHE to simulate the ground state of the transformed Hamiltonian by identifying the Pauli strings in the newly transformed Hamiltonian as observables. To efficiently implement this idea, we require that the number of Pauli strings in \hat{H}' scale polynomially with the system size n . This requirement restricts the possible forms of gauge transformation for \hat{W} . For local Hamiltonian such as quantum spin models, \hat{W} can be in the form of single-qubit rotation gates $\hat{W} = \prod_i \exp(i\tau_i P_i)$, where P_i is the Pauli gate X, Y or Z.

From a theoretical perspective, we now have the energy estimation as:

$$\begin{aligned} \langle \hat{H} \rangle &= \text{Tr} \left(\hat{f}_\phi \rho_\theta \hat{f}_\phi^\dagger (\hat{W}_\tau^\dagger \hat{H} \hat{W}_\tau) \right) / \text{Tr} \left(\hat{f}_\phi \rho_\theta \hat{f}_\phi^\dagger \right) \\ &= \text{Tr} \left((\hat{W}_\tau \hat{f}_\phi) \rho_\theta (\hat{W}_\tau \hat{f}_\phi)^\dagger \hat{H} \right) / \text{Tr} \left(\hat{f}_\phi \rho_\theta \hat{f}_\phi^\dagger \right). \end{aligned} \quad (5)$$

Therefore, the transformed Hamiltonian setup with VQNHE essentially gives a more powerful variational post-processing channel than the plain diagonal matrix \hat{f} . The new effective post-processing channel is $\hat{W}_\tau \hat{f}_\phi$, which has non-vanishing off-diagonal contributions. The

enhanced post-processing capacity implies better performance on ground state energy optimization and quantum error mitigation. A limit is when \hat{W} is a diagonal transformation for the original Hamiltonian H , i.e., the transformed Hamiltonian \hat{H}' is a diagonal matrix. In that case, we can train a diagonal f to successfully project the PQC output ρ to the exact ground state and thus free from any quantum noise.

In the plain VQE, such a transformed Hamiltonian approach can be directly implemented on the circuit, and there is no need to track the new transformed Hamiltonian. However, in the VQNHE setup, such gauge transformation cannot be implemented on the circuit as there is an uncommutable neural module in between. The order in our approach is: PQC U_θ + neural post-processing f_ϕ + gauge transformation \hat{W}_τ . If we naively implement the gauge transformation on the circuit, the order is instead PQC U_θ + gauge transformation W_τ + neural post-processing f_ϕ . In the latter order, the gauge transformation is trivial, as it can be absorbed into the PQC itself.

We still consider the five-qubit TFIM as a specific example to demonstrate the workflow and illustrate the benefits of the transformed Hamiltonian approach. We take the gauge transformation $\hat{W} = \prod_i \exp(i\tau_i Y_i)$, and the corresponding transformed Hamiltonian is

$$\begin{aligned} \hat{H}'_\tau &= \sum_i (\cos 2\tau_i \cos 2\tau_{i+1} Z_i Z_{i+1} + \sin 2\tau_i \sin 2\tau_{i+1} X_i X_{i+1} \\ &\quad - \sin 2\tau_i \cos 2\tau_{i+1} X_i Z_{i+1} - \cos 2\tau_i \sin 2\tau_{i+1} Z_i X_{i+1} \\ &\quad - \cos 2\tau_i X_i - \sin 2\tau_i Z_i), \end{aligned} \quad (6)$$

which contains a polynomial number of Pauli string terms. We utilize the PQC ansatz of a layered form [H, ZZ, Rx, XX, Ry] (See the SM for ansatz notation).

With the introduction of the transformed Hamiltonian on top of the VQNHE setup, we are now equipped with more options on noisy adaptive retraining. We run adaptive retraining for all combinations of **q**uantum module, **n**eural module and **t**ransformation module. The energy after each kind of retraining is displayed in Fig. 3. It is worth noting that the line for the quantum-only retraining also nearly coincides with the line of no retraining and retraining on quantum and transformation parts (not shown), since the quantum part itself cannot be tuned to minimize the depolarizing error as we mentioned before, and the transformation part can be absorbed into the last layer of Ry in the PQC trivially when the neural module is fixed to identity.

The most crucial insights from Fig. 3 are that the $n+t$ retraining delivers a similar QEM performance as the joint retraining ($q+n$), and that the QEM capacity for the $n+t$ retraining is even stronger than the conventional joint retraining ($q+n$) when the overall noise strength is high. Since the PQC is fixed in the $n+t$ retraining scheme, we can carry out the fast biased retrain-

ing. Therefore, the classically tractable biased retraining combining the neural post-processing and parameterized Hamiltonian transformation can achieve competitive QEM results as joint retraining but avoid issues such as finite sampling errors or quantum gradient vanishing (barren plateau issue). We also report the transformed Hamiltonian approach on the Heisenberg model and obtain even better error mitigation results. (See the Supplemental Material for details.)

Discussions: The proposed QEM scheme in this work is very promising as it requires fewer hardware resources compared to other well-established QEM schemes. The advantage of resource efficiency is especially prominent for the biased retraining, which only requires the same amount of measurement shots and hardware resources as one round energy estimation. On the contrary, zero noise extrapolation (ZNE) [14, 15], one of the most common QEM techniques, needs to be conducted on the hardware of different noise strengths. Besides, if we fix the PQC weights, then the zero noise extrapolation limit is biased since the PQC is suboptimal in the noiseless limit. Moreover, virtual distillation method [24–27], which prepares multiple copies of the state, and quasi-probability method [15, 29], which requires tomography on the gates, take much more hardware resources and running times.

Two further comments are in order. Firstly, our QEM proposal is strongly correlated with the VQNHE setup and rooted in energy variational principle. Therefore, the current proposal is not a universal error mitigation method for any circuits. Secondly, the current QEM scheme can be easily combined with other error mitigation techniques for VQNHE. Since most QEM schemes focus on the error mitigation for the expectation values (from PQC) of some observables, they are compatible with the adaptive retraining for VQNHE. Specifically, we have successfully combined a technique of readout error mitigation with the retraining scheme (see the results in Supplemental Material).

Conclusion: In this work, we investigate the baked-in QEM scheme for VQNHE and demonstrate that the adaptive retraining manifests excellent error-mitigating effects. We then analyze the QEM capacity and present theoretical explanations for various scaling relations observed in experiments. In addition, we propose an enhancement add-on for VQNHE: the transformed Hamiltonian approach. Using the parameterized gauge Hamiltonian, VQNHE shows even better expressive power and QEM capability.

Acknowledgements: This work is supported in part by the NSFC under Grant No. 11825404 (SXZ, ZQW, and HY), the MOSTC under Grants No. 2018YFA0305604 and No. 2021YFA1400100 (HY), the CAS Strategic Priority Research Program under Grant No. XDB28000000 (HY), and Beijing Municipal Science and Technology Commission under Grant No. Z181100004218001 (HY).

Note Added: After the completion of this work, we notice an interesting paper [52] on related topics. This paper shares some similarities with the tri-optimization part in our work. While Ref. [52] utilizes a bi-optimization setup of combining Heisenberg transformed Hamiltonian with variational quantum circuit, the present work employs a tri-optimization setup combining Heisenberg transformed Hamiltonian (potentially nonunitary), variational quantum circuit, and additionally neural networks in the middle with help of VQNHE, which in general has larger expressive power.

* kimhsieh@tencent.com

† yaohong@tsinghua.edu.cn

‡ shengy Zhang@tencent.com

- [1] M. Cerezo, A. Arrasmith, R. Babbush, S. C. Benjamin, S. Endo, K. Fujii, J. R. McClean, K. Mitarai, X. Yuan, L. Cincio, and P. J. Coles, Variational quantum algorithms, *Nature Reviews Physics* **3**, 625 (2021).
- [2] K. Bharti, A. Cervera-Lierta, T. H. Kyaw, T. Haug, S. Alperin-Lea, A. Anand, M. Degroote, H. Heimonen, J. S. Kottmann, T. Menke, W.-K. Mok, S. Sim, L.-C. Kwek, and A. Aspuru-Guzik, Noisy intermediate-scale quantum (NISQ) algorithms, *arXiv:2101.08448* (2021).
- [3] S. Endo, Z. Cai, S. C. Benjamin, and X. Yuan, Hybrid Quantum-Classical Algorithms and Quantum Error Mitigation, *Journal of the Physical Society of Japan* **90**, 032001 (2021).
- [4] F. Arute, K. Arya, R. Babbush, D. Bacon, J. C. Bardin, R. Barends, R. Biswas, S. Boixo, F. G. S. L. Brandao, D. A. Buell, B. Burkett, Y. Chen, Z. Chen, B. Chiaro, R. Collins, W. Courtney, A. Dunsworth, E. Farhi, B. Foxen, A. Fowler, C. Gidney, M. Giustina, R. Graff, K. Guerin, S. Habegger, M. P. Harrigan, M. J. Hartmann, A. Ho, M. Hoffmann, T. Huang, T. S. Humble, S. V. Isakov, E. Jeffrey, Z. Jiang, D. Kafri, K. Kechedzhi, J. Kelly, P. V. Klimov, S. Knysh, A. Korotkov, F. Kostritsa, D. Landhuis, M. Lindmark, E. Lucero, D. Lyakh, S. Mandrà, J. R. McClean, M. McEwen, A. Megrant, X. Mi, K. Michielsen, M. Mohseni, J. Mutus, O. Naaman, M. Neeley, C. Neill, M. Y. Niu, E. Ostby, A. Petukhov, J. C. Platt, C. Quintana, E. G. Rieffel, P. Roushan, N. C. Rubin, D. Sank, K. J. Satzinger, V. Smelyanskiy, K. J. Sung, M. D. Trevithick, A. Vainsencher, B. Villalonga, T. White, Z. J. Yao, P. Yeh, A. Zalcman, H. Neven, and J. M. Martinis, Quantum supremacy using a programmable superconducting processor, *Nature* **574**, 505 (2019).
- [5] H.-S. Zhong, H. Wang, Y.-H. Deng, M.-C. Chen, L.-C. Peng, Y.-h. Luo, J. Qin, D. Wu, X. Ding, Y. Hu, P. Hu, X.-y. Yang, W.-j. Zhang, H. Li, Y. Li, X. Jiang, L. Gan, G. Yang, L. You, Z. Wang, L. Li, N.-l. Liu, C.-y. Lu, and J.-w. Pan, Quantum computational advantage using photons, *Science* **370**, 1460 (2020).
- [6] J. Preskill, Quantum Computing in the NISQ era and beyond, *Quantum* **2**, 79 (2018).
- [7] A. Peruzzo, J. McClean, P. Shadbolt, M.-H. Yung, X.-Q. Zhou, P. J. Love, A. Aspuru-Guzik, and J. L. O’Brien, A variational eigenvalue solver on a photonic quantum

- processor, *Nature Communications* **5**, 4213 (2014).
- [8] P. J. J. O'Malley, R. Babbush, I. D. Kivlichan, J. Romero, J. R. McClean, R. Barends, J. Kelly, P. Roushan, A. Tranter, N. Ding, B. Campbell, Y. Chen, Z. Chen, B. Chiaro, A. Dunsworth, A. G. Fowler, E. Jeffrey, E. Lucero, A. Megrant, J. Y. Mutus, M. Neeley, C. Neill, C. Quintana, D. Sank, A. Vainsencher, J. Wenner, T. C. White, P. V. Coveney, P. J. Love, H. Neven, A. Aspuru-Guzik, and J. M. Martinis, Scalable Quantum Simulation of Molecular Energies, *Physical Review X* **6**, 031007 (2016).
 - [9] J. R. McClean, J. Romero, R. Babbush, and A. Aspuru-Guzik, The theory of variational hybrid quantum-classical algorithms, *New Journal of Physics* **18**, 023023 (2016).
 - [10] J.-G. Liu, Y.-H. Zhang, Y. Wan, and L. Wang, Variational quantum eigensolver with fewer qubits, *Physical Review Research* **1**, 023025 (2019).
 - [11] S. McArdle, S. Endo, A. Aspuru-Guzik, S. C. Benjamin, and X. Yuan, Quantum computational chemistry, *Reviews of Modern Physics* **92**, 015003 (2020).
 - [12] H. R. Grimsley, S. E. Economou, E. Barnes, and N. J. Mayhall, An adaptive variational algorithm for exact molecular simulations on a quantum computer, *Nature Communications* **10**, 3007 (2019).
 - [13] C. Y. Hsieh, Q. Sun, S. Zhang, and C. K. Lee, Unitary-coupled restricted Boltzmann machine ansatz for quantum simulations, *npj Quantum Information* **7**, 19 (2021).
 - [14] Y. Li and S. C. Benjamin, Efficient Variational Quantum Simulator Incorporating Active Error Minimization, *Physical Review X* **7**, 021050 (2017).
 - [15] K. Temme, S. Bravyi, and J. M. Gambetta, Error Mitigation for Short-Depth Quantum Circuits, *Physical Review Letters* **119**, 180509 (2017).
 - [16] S. Endo, S. C. Benjamin, and Y. Li, Practical Quantum Error Mitigation for Near-Future Applications, *Physical Review X* **8**, 031027 (2018).
 - [17] A. Kandala, K. Temme, A. D. Córcoles, A. Mezzacapo, J. M. Chow, and J. M. Gambetta, Error mitigation extends the computational reach of a noisy quantum processor, *Nature* **567**, 491 (2019).
 - [18] C. Song, J. Cui, H. Wang, J. Hao, H. Feng, and Y. Li, Quantum computation with universal error mitigation on a superconducting quantum processor, *Science Advances* **5**, eaaw5686 (2019).
 - [19] S. McArdle, X. Yuan, and S. Benjamin, Error-Mitigated Digital Quantum Simulation, *Physical Review Letters* **122**, 180501 (2019).
 - [20] Y. Chen, M. Farahzad, S. Yoo, and T.-C. Wei, Detector tomography on IBM quantum computers and mitigation of an imperfect measurement, *Physical Review A* **100**, 052315 (2019).
 - [21] F. B. Maciejewski, Z. Zimborás, and M. Oszmaniec, Mitigation of readout noise in near-term quantum devices by classical post-processing based on detector tomography, *Quantum* **4**, 257 (2020).
 - [22] S. Bravyi, S. Sheldon, A. Kandala, D. C. McKay, and J. M. Gambetta, Mitigating measurement errors in multiqubit experiments, *Physical Review A* **103**, 042605 (2021).
 - [23] G. S. Barron and C. J. Wood, Measurement Error Mitigation for Variational Quantum Algorithms, *arXiv:2010.08520* (2020).
 - [24] B. Koczor, Exponential Error Suppression for Near-Term Quantum Devices, *Physical Review X* **11**, 031057 (2021).
 - [25] W. J. Huggins, S. McArdle, T. E. O'Brien, J. Lee, N. C. Rubin, S. Boixo, K. B. Whaley, R. Babbush, and J. R. McClean, Virtual Distillation for Quantum Error Mitigation, *Physical Review X* **11**, 041036 (2021).
 - [26] M. Huo and Y. Li, Dual-state purification for practical quantum error mitigation, *arXiv:2105.01239* (2021).
 - [27] B. Koczor, The Dominant Eigenvector of a Noisy Quantum State, *arXiv:2104.00608* (2021).
 - [28] P. Czarnik, A. Arrasmith, P. J. Coles, and L. Cincio, Error mitigation with Clifford quantum-circuit data, *Quantum* **5**, 592 (2021).
 - [29] A. Strikis, D. Qin, Y. Chen, S. C. Benjamin, and Y. Li, Learning-based quantum error mitigation, *arXiv:2005.07601* (2020).
 - [30] L. Cincio, K. Rudinger, M. Sarovar, and P. J. Coles, Machine Learning of Noise-Resilient Quantum Circuits, *PRX Quantum* **2**, 010324 (2021).
 - [31] A. Zlokapa and A. Gheorghiu, A deep learning model for noise prediction on near-term quantum devices, *arXiv:2005.10811* (2020).
 - [32] A. Lowe, M. H. Gordon, P. Czarnik, A. Arrasmith, P. J. Coles, and L. Cincio, Unified approach to data-driven quantum error mitigation, *arXiv:2011.01157* (2020).
 - [33] S.-X. Zhang, C.-Y. Hsieh, S. Zhang, and H. Yao, Differentiable Quantum Architecture Search, *arXiv:2010.08561* (2020).
 - [34] P. Suchsland, F. Tacchino, M. H. Fischer, T. Neupert, P. K. Barkoutsos, and I. Tavernelli, Algorithmic Error Mitigation Scheme for Current Quantum Processors, *Quantum* **5**, 492 (2021).
 - [35] D. Bultrini, M. H. Gordon, P. Czarnik, A. Arrasmith, P. J. Coles, and L. Cincio, Unifying and benchmarking state-of-the-art quantum error mitigation techniques, *arXiv:2107.13470* (2021).
 - [36] A. A. Zhukov and W. V. Pogosov, Quantum error reduction with deep neural network applied at the post-processing stage, *arXiv:2105.07793* (2021).
 - [37] E. R. Bennewitz, F. Hopfmueller, B. Kulchytskyy, J. Carrasquilla, and P. Ronagh, Neural Error Mitigation of Near-Term Quantum Simulations, *arXiv:2105.08086* (2021).
 - [38] S.-X. Zhang, Z.-Q. Wan, C.-K. Lee, C.-Y. Hsieh, S. Zhang, and H. Yao, Variational Quantum-Neural Hybrid Eigensolver, *arXiv:2106.05105* (2021).
 - [39] R. Jastrow, Many-body problem with strong forces, *Physical Review* **98**, 1479 (1955).
 - [40] G. Mazzola, P. J. Ollitrault, P. K. Barkoutsos, and I. Tavernelli, Nonunitary Operations for Ground-State Calculations in Near-Term Quantum Computers, *Physical Review Letters* **123**, 130501 (2019).
 - [41] F. Benfenati, G. Mazzola, C. Capecchi, P. K. Barkoutsos, P. J. Ollitrault, I. Tavernelli, and L. Guidoni, Improved accuracy on noisy devices by non-unitary Variational Quantum Eigensolver for chemistry applications, *arXiv:2101.09316* (2021).
 - [42] G. Carleo and M. Troyer, Solving the quantum many-body problem with artificial neural networks, *Science* **355**, 602 (2017).
 - [43] D.-L. Deng, X. Li, and S. Das Sarma, Machine learning topological states, *Physical Review B* **96**, 195145 (2017).
 - [44] G. Carleo, Y. Nomura, and M. Imada, Constructing exact representations of quantum many-body systems with deep neural networks, *Nature Communications* **9**, 5322 (2018).

- (2018).
- [45] Z. Cai and J. Liu, Approximating quantum many-body wave functions using artificial neural networks, *Physical Review B* **97**, 035116 (2018).
 - [46] D. Pfau, J. S. Spencer, A. G. d. G. Matthews, and W. M. C. Foulkes, Ab initio solution of the many-electron Schrödinger equation with deep neural networks, *Physical Review Research* **2**, 033429 (2020).
 - [47] J. Hermann, Z. Schätzle, and F. Noé, Deep-neural-network solution of the electronic Schrödinger equation, *Nature Chemistry* **12**, 891 (2020).
 - [48] S.-X. Zhang, Z.-Q. Wan, and H. Yao, Automatic Differentiable Monte Carlo: Theory and Application, *arXiv:1911.09117* (2019).
 - [49] J. R. McClean, S. Boixo, V. N. Smelyanskiy, R. Babush, and H. Neven, Barren plateaus in quantum neural network training landscapes, *Nature Communications* **9**, 4812 (2018).
 - [50] S. Wang, E. Fontana, M. Cerezo, K. Sharma, A. Sone, L. Cincio, and P. J. Coles, Noise-induced barren plateaus in variational quantum algorithms, *Nature Communications* **12**, 6961 (2021).
 - [51] M. Cerezo, A. Sone, T. Volkoff, L. Cincio, and P. J. Coles, Cost function dependent barren plateaus in shallow parametrized quantum circuits, *Nature Communications* **12**, 1791 (2021).
 - [52] Z.-X. Shang, M.-C. Chen, X. Yuan, C.-Y. Lu, and J.-W. Pan, Schrödinger-Heisenberg Variational Quantum Algorithms, *arXiv:2112.07881* (2021).

SUPPLEMENTAL MATERIALS

Single qubit example in detail: VQNHE, QEM and more

The motivations behind the calculation on the one-qubit system are: (1) the system is simple enough to be analytically traced and free from local minimum issue for retraining analysis since the number of trainable parameters is very limited, and (2) the system is still powerful enough for illustrating general features and providing insights on a general picture of the inherent QEM capacity of VQNHE.

Specifically, we consider a system Hamiltonian defined on single qubit as $\hat{H} = X + Z$ whose ground state is analytically given as $|\psi_0\rangle \propto (1 - \sqrt{2}, 1)$ with the ground state energy $-\sqrt{2}$. We consider the depolarizing noise channel, where the ideal ground state density matrix $\rho_0 = |\psi_0\rangle\langle\psi_0|$ is transformed to $\rho = (1 - p)\rho_0 + pI/2^n$. For an one-qubit system, the post-processing module f has only one freedom $r = (f(1) - f(0))/(f(1) + f(0))$, note that the notation here is slightly different from the main text and the post-processing matrix is defined as

$$\hat{f} = \begin{pmatrix} 1-r & 0 \\ 0 & 1+r \end{pmatrix}. \quad (S1)$$

The PQC in this example contains only one $\text{Ry}(\theta)$ rotation gate and thus the output wavefunction from the PQC without quantum noise is in the form of $(\cos(\theta), -\sin(\theta))$. The output density matrix in the presence of depolarizing quantum noise of strength p is in the form of

$$\rho = \begin{pmatrix} p/2 + (1-p)\cos^2\theta & (p-1)\cos\theta\sin\theta \\ (p-1)\cos\theta\sin\theta & p/2 + (1-p)\sin^2\theta \end{pmatrix}. \quad (S2)$$

The final effective density matrix after VQNHE post-processing is $\rho_{\text{eff}} = \hat{f}\rho\hat{f}/\text{Tr}(\hat{f}\rho\hat{f})$. With $p = 0$ and $r = 0$, we obtain the optimal parameters as $\theta_0 = -\arctan(1/(1 - \sqrt{2})) \approx 1.178$ and the corresponding energy coincides with the exact value $-\sqrt{2} \approx -1.414$. With the noise $p > 0$ turned on, the energy estimation with original weights is $E_{r_0, \theta_0} = -\sqrt{2} + \sqrt{2}p$. If only θ from the PQC is allowed to be retrained, the energy estimation cannot be improved. If only r is allowed to be retrained, the optimal r with noise and the corresponding energy estimation is given as $E_r = -\frac{\sqrt{2}(p+1)}{2p+1} \approx -2\sqrt{2}p^2 + \sqrt{2}p - \sqrt{2}$ when $p \ll 1$, where the optimal new $r = \sqrt{2}p$. Therefore, the retraining energy gain is quadratic with the error strength $\delta E = E_r - E_{r_0} = -2\sqrt{2}p^2$.

We further consider the case when both r and θ can be further tuned on noisy hardware. In this case, the retrained energy estimation is $E_{r, \theta} \approx -\sqrt{2} + \frac{\sqrt{2}}{2}p$. Therefore, the QEM energy gain after joint retraining is $\delta E = E_{r, \theta} - E_{r_0, \theta_0} = -\frac{\sqrt{2}}{2}p$ which is better than retraining on the neural network only and shows linear scaling with the noise strength. In this case, the optimal parameters under noise is $\theta = \pi/4$ and $r = 1/(1 - p + \sqrt{2 - 2p + p^2}) \approx \left(1 - \frac{1}{\sqrt{2}}\right)p + \sqrt{2} - 1$. It is worth noting that the noise-aware optimal parameters here are not connected to the optimal parameter we have in the noise-free setup when $p \rightarrow 0$. This is the key for the linear scaling relation since we have proved any parameters adiabatically connected to the ideal case only contributes to quadratic scaling for the QEM capacity.

In summary, the simple one-qubit example covers some of the main results in this work, including the scaling relation between the energy gain and the error strength as well as the reason behinds such scaling relations.

Finally we investigate error-mitigated estimation on other observables instead of energy in the VQNHE setup. As we will show now, the retraining QEM scheme for VQNHE performs sub-optimally at predicting other observables and this is a general feature for variational wavefunction ansatz and not unique to our scheme. We focus on the observable X and Z , the exact expectation is $\langle X \rangle = \langle Z \rangle = -1/\sqrt{2}$. In the presence of noise, the expectation under the noise-free optimal parameters are $\langle X \rangle = \frac{-1+p}{\sqrt{2}}$ and $\langle Z \rangle = \frac{-1+p}{\sqrt{2}}$. With the noise and neural only retrained parameters, we have the estimated expectation $\langle X \rangle = -\frac{(p-1)(2p^2-1)}{\sqrt{2}(2p+1)} \approx -1/\sqrt{2} + 3p/\sqrt{2} - 2\sqrt{2}p^2$ and $\langle Z \rangle = \frac{p(2(p-1)p-3)-1}{\sqrt{2}(2p+1)} \approx -1/\sqrt{2} - p/\sqrt{2}$. Note the estimation on other observables' expectation does not get closer to the exact value after retraining. Namely, the retraining QEM strategy here is not suitable for error mitigation on other observables than the Hamiltonian operator. In addition, with joint retraining, the estimated expectation becomes $\langle X \rangle = -\frac{2}{(\sqrt{p^2-2p+2-p+1})\left(\frac{1}{(\sqrt{p^2-2p+2-p+1})^2+1}\right)} \approx -1/\sqrt{2} + 3p/(2\sqrt{2})$ and $\langle Z \rangle = -\frac{2}{(\sqrt{p^2-2p+2-p+1})\left(\frac{1}{(\sqrt{p^2-2p+2-p+1})^2+1}\right)} \approx -1/\sqrt{2} - p/(2\sqrt{2})$. Again, the deviation of the estimation is worse, though slightly better than post-processing only retraining.

	retraining energy gain	deviation of X	deviation of Z
noise-free opt params	0	$p/\sqrt{2}$	$p/\sqrt{2}$
neural only retraining	$-2\sqrt{2}p^2$	$3p/\sqrt{2} - 2\sqrt{2}p^2$	$-p/\sqrt{2}$
joint retraining	$-1/\sqrt{2}p$	$3p/(2\sqrt{2})$	$-p/(2\sqrt{2})$

TABLE S1. VQNHE-QEM results for one qubit system of Hamiltonian $\hat{H} = X + Z$ under depolarizing noise $p \ll 1$.

	retraining energy gain	deviation of X	deviation of Z
noise-free opt params	0	$1/(2\sqrt{2})\gamma$	$(1 + 1/\sqrt{2})\gamma$
neural only retraining	$-\frac{(121+84\sqrt{2})}{16\sqrt{2}}\gamma^2$	$\frac{3}{8}(4 + 3\sqrt{2})\gamma$	$-\frac{1}{8}(4 + 3\sqrt{2})\gamma$
joint retraining	$-\left(1 + \frac{3}{2\sqrt{2}}\right)\gamma$	0	0

TABLE S2. VQNHE-QEM results for one qubit system of Hamiltonian $\hat{H} = X + Z$ under amplitude damping noise $\gamma \ll 1$.

Indeed, the variational wavefunction giving the minimal energy estimation is not guaranteed to give the most accurate expectations for other observables. Only when there is no noise and the variational expressive power is good enough, the variational wavefunction can approach the exact ground state wavefunction as close as possible, the estimation on other observables from such variational wavefunctions then become reliable. And this is not the case here, as the noise intrinsically forbids VQNHE to provide a sufficiently accurate approximation of the desired ground state under certain cases. In other words, in the restricted Hilbert space accessible to VQNHE (limited by the noise, ansatz circuit, and choices of the neural network, etc.) for approximating the ground state, the state giving the lowest energy estimation does not necessarily coincide with the state giving the most accurate estimation on a given observable not commutable with the Hamiltonian operator. However, we stress that a worse estimation on another observable (other than the Hamiltonian) is not a unique side effect brought by our QEM scheme or quantum-neural hybrid state. Instead, this exact phenomenon exists for all variational algorithms in principle. The results for QEM energy gain and observable deviation before and after retraining in the presence of depolarizing noise are summarized in Table S1.

We further consider another example: still the same system but the quantum circuit is subject to the influence of amplitude damping error channels instead. The Kraus operators for such error are defined as

$$K_0 = \begin{pmatrix} 1 & 0 \\ 0 & \sqrt{1-\gamma} \end{pmatrix}, \quad K_1 = \begin{pmatrix} 0 & \sqrt{\gamma} \\ 0 & 0 \end{pmatrix}, \quad (\text{S3})$$

and the density operator in the presence of noise is $\rho = \sum_i K_i \rho_0 K_i^\dagger$.

The energy estimation with the noise-free optimal parameters is $E_{r_0, \theta_0} = \frac{1}{2}((2 + \sqrt{2})\gamma - \sqrt{2}(\sqrt{1-\gamma} + 1)) \approx (1 + 3/(2\sqrt{2}))\gamma - \sqrt{2}$. As we can see, the energy deviation affected by the noise is still linear with γ in the leading order, namely, γ here characterizes the strength of the amplitude damping error, playing a similar role as p in depolarizing channel. Meanwhile, the observable estimation with the ideal parameters are $\langle X \rangle = -\sqrt{1-\gamma}/\sqrt{2} \approx -1/\sqrt{2} + \gamma/(2\sqrt{2})$ and $\langle Z \rangle = -1/\sqrt{2} + (1 + 1/\sqrt{2})\gamma$.

The energy gain by retraining only on the neural part (tuning r) is

$$\delta E = -\frac{1}{2}(2 + \sqrt{2})\gamma + \frac{\sqrt{1-\gamma}}{\sqrt{2}} - \sqrt{\frac{1}{2\sqrt{2}\gamma + 3\gamma + 1} + 1} + \frac{1}{\sqrt{2}} = -\frac{(121 + 84\sqrt{2})\gamma^2}{16\sqrt{2}} + O(\gamma^3)$$

, where the optimal $r \approx (3/2 + 7\sqrt{2}/8)\gamma$ is adiabatically connect to $r = 0$ when $\gamma \rightarrow 0$. The estimated expectation for other observables X and Z after retraining are $\langle X \rangle \approx \frac{3}{8}(4 + 3\sqrt{2})\gamma - \frac{1}{\sqrt{2}}$ and $\langle Z \rangle \approx \frac{1}{8}(-4 - 3\sqrt{2})\gamma - \frac{1}{\sqrt{2}}$, respectively.

Namely, the energy gain is still quadratic with the error strength. If the joint retraining is allowed, the energy can be fully recovered to the noiseless exact value. In this case, the estimated expectations for other observables are also exact. The gain part is thus linear with γ as: $\delta E = -\left(1 + \frac{3}{2\sqrt{2}}\right)\gamma$. For the amplitude-damping channels, we find the scalings coincide perfectly with those for the case of depolarizing channel. Hence, we argue the universality of these QEM scaling relations. The results for QEM energy gain and observable deviation before and after retraining with the presence of amplitude damping noise are summarized in S2.

Scaling results on biased neural retraining

We first recapitulate the setup for the biased neural retraining and explain why it is important to investigate the scaling between the biased retraining energy gain and the number of measurement shots required. For unbiased retraining, in each round of retraining optimization, we must take k shots of measurement to ensure the sampling errors on quantum expectation and quantum gradient estimation are all under an acceptable threshold. In general, we need $t = O(10^3)$ optimization rounds to ensure the convergence of the energy estimations. Therefore, the total number of measurement shots required for unbiased training is $M = kt$ which may be very demanding on quantum resources in the NISQ era. Instead, for optimizations on the classical module such as the neural part or the transformation part in the transformed Hamiltonian approach, we can run the so-called biased retraining procedure, where only $M = k$ measurement shots are executed, and these k bitstrings are utilized for each optimization round since the PQC does not change during the neural retraining. In other words, besides the k measurement shots at the beginning of the biased retraining, all other workloads are done classically, rendering a much stable and light retraining procedure.

However, the biased retraining workflow is **biased**. Since k measurement shots collected at the beginning can be biased due to the fine sampling errors, such bias may aggravate by the variational optimization. Namely, the retraining may overfit the biased quantum results and overestimate the QEM capacity. We must investigate the scaling between energy gain and the number of measurement shots carefully, so that we can differentiate the intrinsic QEM contribution from the biased overfitting contribution.

To identify the intrinsic QEM capability from biased retraining, we first run the same PQC N times ($N = 819200$ for cases below unless specified) and save the corresponding sets of bitstrings. We then compute the energy gain averaged over retraining on randomly selected $N/100$ or $N/10$ bitstrings. Together with the energy retraining gain from the full set N bitstrings, we find the average energy gain δE scaling with the number of measurement shots required in the biased retraining. Since we compute the average energy gain, the measurement uncertainty for the energy estimation is suppressed by the order of $1/\sqrt{819200}$ which can be safely omitted.

We use one-dimensional five-site transverse field Ising model (TFIM) with open boundary condition as VQNHE target Hamiltonian. The Hamiltonian is given as $\hat{H} = \sum_{i=1}^{n-1} Z_i Z_{i+1} - \sum_{i=1}^n X_i$. The PQC is a layered ansatz [H, ZZ, Rx]. We first apply the above scaling analysis on the ideal noise-free simulator. For $N/100, N/10, N$, the retraining energy gains are $-0.030, -0.0036, -0.0003$, respectively. Since we expect no energy gain is possible when the retraining takes place in the noiseless setting, the non-vanishing values originate from overfitting on the biased bitstring results. The scaling relation is $\delta E \propto 1/M$, where M is the number of measurement shots the retraining is based on. In the infinite number of measurement shots limit $M \rightarrow \infty$, zero energy gain after retraining is recovered for the noiseless case.

We further run the same biased retraining scaling analysis on IBM_Santiago noisy simulator. The experiments without readout error mitigation gives the energy gain $-0.0939, -0.0768, -0.0748$ for $N/100, N/10, N$ bitstrings. The scaling is perfectly described by $\delta E = B + A/M$ where $B \approx -0.075$ is the intrinsic QEM part contributing to the energy gain from neural retraining and A/M scaling part gives the overfitting artifact. The same scaling relation applies for noisy simulator results with readout error mitigation and results directly collected from IBM_Santiago hardware.

For IBM_Santiago simulator, after enforcing the readout error mitigation, the raw results are improved and the retraining gain is lower: the gains are $-0.0366, -0.0116, -0.009$ for 8192, 81920, 819200 bitstring results based retraining. The intrinsic QEM offset is around $B \approx -0.009$, less than the case without readout error mitigation in magnitude (-0.075).

We also carry out the scaling analysis experiments on IBM_Santiago hardware, where $8192 * 50$ sets of bitstrings are collected in total. The retrained energy gains without the readout error mitigation are $-0.135, -0.113, -0.112$ for results based on 8192, 81920 and $8192 * 50$ bitstrings, respectively. Again, the effect of retraining on the energy gain still follows the $\delta E = B + A/M$ scaling with intrinsic QEM capacity $B \approx -0.111$.

To further investigate the QEM effect of the retrained VQNHE in the presence of quantum noise, we utilize depolarizing error model, where each two-qubit gate is followed by applying a depolarizing noise of strength p on each qubit. For a given p , say $p = 0.02$, we observe the same overfitting scaling relation between the biased energy gain and the number of measurement shots based. For $N = 8192, 81920, 819200$, we have the energy gain as $-0.0694, -0.0482$ and -0.0464 , respectively, where the scaling relation is approximated by $\delta E \approx -0.046 - A/M$ again.

Finally, we comment that the scaling here is about the average of δE , where the average is taken over different groups composed of M measurement shots. For individual cases, the energy gain retrained on M measurement shots is a random variable, with the mean value scale as $B + A/M$ as indicated before and the standard deviation is in the order $1/\sqrt{M}$, which is the typical behavior due to the finite sampling errors.

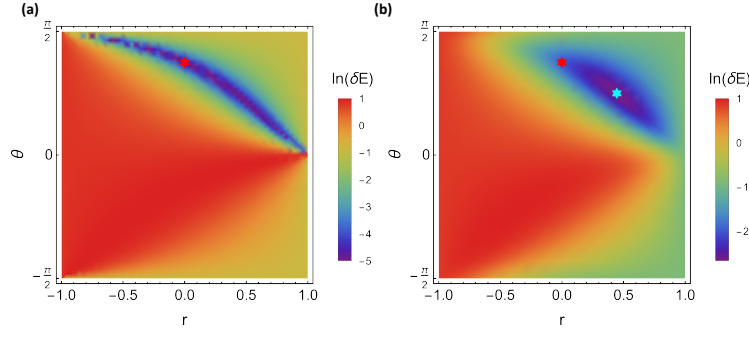


FIG. S1. Energy landscape with varying r and θ for one-qubit system $\hat{H} = X + Z$. The energy is presented in log scale $\ln(E - E_0 + e^{-5})$, where E_0 is the exact ground state energy and E is the energy estimation given circuit parameter θ and neural parameter r . (a) Noiseless case: the red star indicates the ideal solution with $r = 1$. All points in the deep blue region of value -5 are legal optimal solutions. (b) Depolarizing noise case with $p = 0.1$: ideal solutions respond differently with the noise on, and the most noise resilient point is indicated by the cyan star which is not adiabatically connected to the original red star. This non-perturbative nature is the origin of linear scaling for QEM capacity.

Energy landscape for joint retraining

See Fig. S1 on why perturbation understanding fails in the joint retraining scenario and how the introduction of noise breaks the symmetry between different noiseless optimal solutions.

Layered quantum ansatz notation

We use a list notation for layered circuit ansatz as $[A, B, C\dots]$ where each term represents a quantum layer. The layers we utilized in this work include (suppose n qubits for the circuit):

- H for Hadamard layer: $\prod_{i=1}^n H_i$ where H_i is Hadamard gate on the i -th qubit.
- ZZ for ZZ layer: $\prod_{i=1}^{n-1} e^{i\theta_i Z_i Z_{i+1}}$ where θ_i is trainable weights and Z_i is the Pauli Z gate on the i -th qubit. Similar rules apply to XX and YY layer.
- Rz for Rz layer: $\prod_{i=1}^n e^{i\theta_i Z_i}$. Similar rules apply to Rx and Ry layer.
- SWAP for parameterized SWAP layer: $\prod_{i=1}^{n-1} e^{i\theta_i \text{SWAP}_{i,i+1}}$, where $\text{SWAP} = \begin{pmatrix} 1 & 0 & 0 & 0 \\ 0 & 0 & 1 & 0 \\ 0 & 1 & 0 & 0 \\ 0 & 0 & 0 & 1 \end{pmatrix}$.

For example, the parameterized circuit ansatz in the form $[H, ZZ, Rx]$ can be expressed as:

$$U = \prod_{i=1}^n e^{i\theta'_i X_i} \prod_{i=1}^{n-1} e^{i\theta_i Z_i Z_{i+1}} \prod_{i=1}^n H_i. \quad (\text{S4})$$

Nonunitary version of transformed Hamiltonian approach

For the transformed Hamiltonian approach, the transformation can also be nonunitary. For nonunitary \hat{W} , we regard it as the nonunitary operation on the VQNHE output state as $|\psi_W\rangle = \frac{\hat{W}|\psi_f\rangle}{|\hat{W}|\psi_f\rangle|}$. Therefore, the final energy estimation is given by

$$\langle \hat{H} \rangle = \frac{\langle 0^n | U^\dagger \hat{f}^\dagger \hat{W}^\dagger \hat{H} \hat{W} \hat{f} U | 0^n \rangle}{\langle 0^n | U^\dagger \hat{f}^\dagger \hat{W}^\dagger \hat{W} \hat{f} U | 0^n \rangle}. \quad (\text{S5})$$

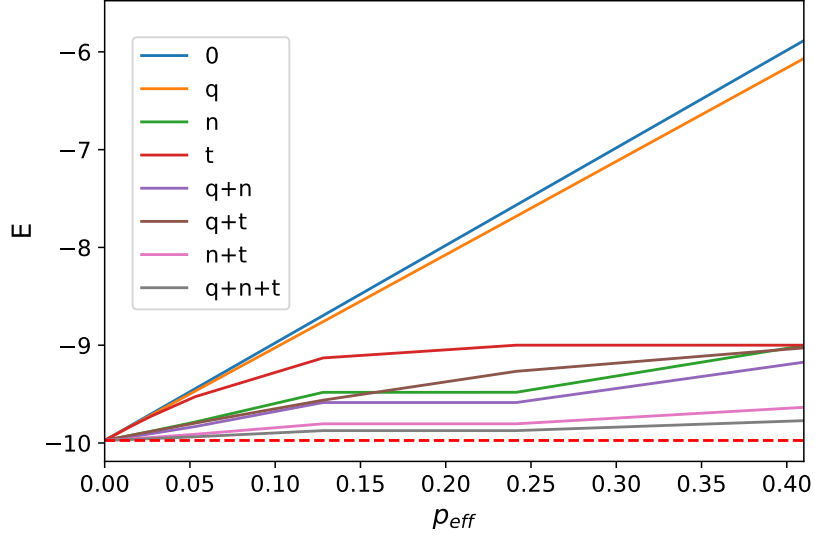


FIG. S2. Transformed Hamiltonian approach on top of VQNHE: QEM results on 1D Heisenberg model with overall depolarizing noise p_{eff} . 0 indicates the energy estimation with noiseless optimal weights (no retraining). q, n, t are for retraining on the PQC, neural network and parameterized transformations, respectively. The dashed line is the exact ground state energy for the simulated system.

In experimental implementations, the nonunitary operation of neural module \hat{f} is simulated by the VQNHE measurement scheme and the nonunitary operation of transformation module \hat{W} is simulated by transforming the Hamiltonian classically. The effective overall nonunitary quantum channel $\hat{W}\hat{f}$ greatly enhances the expressive power and quantum noise resilience of plain VQE where only the quantum circuit U can be tuned. Typical examples for nonunitary transformation are also single-qubit rotations $\exp(i\tau\hat{P})$, but τ can take complex value this time.

Note that we have actually incorporated the nonunitary property of the transformation in the TFIM example in the main text. However, the results after optimization all give zero imaginary part in τ , indicating nonunitary character has no further gain in TFIM + single-qubit rotation transformation case. As we will see, this is not true for Heisenberg model simulation.

Transformed Hamiltonian VQNHE results on Heisenberg model

In this section, we report tri-optimization results on one-dimensional six-sites isotropic Heisenberg model with an open boundary condition, whose Hamiltonian is given by: $\hat{H} = \sum_{i=1}^{n-1} (X_i X_{i+1} + Y_i Y_{i+1} + Z_i Z_{i+1})$. The ground state energy is -9.9743 . Since the system has $SU(2)$ symmetry, we pick the circuit ansatz which also respects such symmetry and thus conserves the total spin J_{tot}^2 . In this case, we adopt a symmetry-preserving PQC layout: [SWAP, SWAP]. Also, we choose a transformation that keeps the symmetry instead of a single-qubit rotation layer. To keep the polynomial overhead for the transformed Hamiltonian, we utilize “half-layer” of parameterized SWAP as the transformation. Specifically, the parameterized transformation we utilized is:

$$\hat{W}_\tau = \prod_{i=1,3,5} e^{i\tau_i \text{SWAP}_{i,i+1}}, \quad (\text{S6})$$

where τ can take complex values as explained in the above section. Such transformation has geometrically compatible gates which are classically tractable and leads to a transformed Hamiltonian containing polynomial number of local terms.

Apart from the new choice on the parameterized transformation, we also allow the post-processing neural model to output complex values, which further enhances the power of the whole setup. We still consider the same type of quantum noise: depolarizing channel attached after each two-qubit gate. And the optimized results with different retraining strategies are shown in Fig. S2.

Fig. S2 conveys a few important messages. Firstly, we again validate that a pure retraining on the PQC gains very little, which supports our conclusion that the noise robustness is unique to VQNHE instead of VQE. Secondly, the

half layered parameterized SWAP transformation is very powerful as it is implemented classically without noise while keeping the quantum state in the correct symmetry factor. The mitigated energy is at least $E = -9$ since even for the fully mixed state $\rho = I/2^n$, the transformation, as a quantum channel effectively, can project the system to an averaged energy -9 . Lastly, we again observe that while triple retraining gives the best error mitigation capacity, the pure classical optimization with n+t is still good enough and even outperforms q+n retraining. Therefore, we can run biased retraining on n+t very fast and obtain much more reliable energy estimations without using too many additional quantum resources.

Hyperparameter settings

Most numerical simulations in this work are conducted using the tensor network based differentiable quantum simulator: `tensorcircuit` (<https://github.com/refraction-ray/tensorcircuit>). We use density matrix simulator to exactly characterize the behavior for the quantum noise.

The neural model for post-processing in VQNHE is a simple fully connected neural network with the output range $[1/e, e]$. The detailed choice of the model is irrelevant since the model easily has full expressive power for the small system size we simulated in this work. For the complex-valued post-processing module we tested in tri-optimization setup on Heisenberg model, we simply utilized a 2^n -dimensional complex-valued variational vector f as the post-processing model. Note that we don't impose the output range restriction in this complex valued case, which may lead to better error mitigation results.

In the tri-optimization setup, the three sets of parameters are updated simultaneously. We apply three Adam optimizers with learning rates 0.005, 0.01 and 0.003 on quantum module, neural module and transformation module, respectively. The convergence of the optimization usually takes thousands of epochs from random initialization.

The initialization on both the PQC and the transformation parameters are drawn from Gaussian distribution with zero mean and small standard deviations, say 0.1.